

## Supplementary information for:

### Quantum Mechanics/Molecular Mechanics Study of Resting-State Vanadium Nitrogenase: Molecular and Electronic Structure of the Iron–Vanadium Cofactor

Bardi Benediktsson<sup>a</sup> and Ragnar Bjornsson<sup>a,b\*</sup>

<sup>a</sup>Science Institute, University of Iceland, Dunhagi 3, 107 Reykjavik, Iceland

<sup>b</sup>Max-Planck Institute for Chemical Energy Conversion, Stiftstrasse 34-36, 45470 Mülheim an der Ruhr, Germany.

## Contents

Computational Details.....	1
Single Point Broken Symmetry Solutions Comparison.....	5
Mulliken spin populations of the 181 QM-atom QM/MM optimized structures.....	14
Mulliken spin populations of all 35 BS solutions for different FeVco models: Single-point QM/MM calculations using X-ray structure.....	15
Mayer bond orders for FeMoco and FeVco.....	23
Localized Orbital Analysis of FeVco.....	24
The BS7 solutions: FeMoco vs. FeVco.....	26
Protonation state of homocitrate.....	28
Protonated FeVco.....	28
Unbound electrons.....	29
New QM/MM model with bulk water.....	31

## Computational Details

**Force field parameters.** The CHARMM36 protein force field<sup>1</sup> was used in all MM and QM/MM calculations. As no forcefield parameters are available for FeVco, atomic charges were derived from Hirshfeld population analysis using the  $[\text{VFe}_7\text{S}_8\text{C}(\text{CO}_3)]^{2-}$  charge configuration and crystal structure geometry for FeVco with relaxed protons (both extended carboxylate arms of FeVco were protonated, making the model 61 QM atoms in total) from a calculation performed with ORCA version 3.0.3 with TPSSh and Ahlrichs def2 triple- $\zeta$  basis set on V, Fe and S but def2 double- $\zeta$  basis set on other atoms and the protein matrix approximated with COSMO<sup>2</sup> ( $\epsilon = 4$ ). Same parameters were used for the P-cluster as in a previous study by us.<sup>3</sup> Lennard-Jones parameters were only added to inorganic sulfides (CHARMM atomtype SM used) and not to metals<sup>4</sup>. Forcefield parameters for homocitrate were adapted from those already available for citrate.<sup>5</sup> Water was modelled as TIP3P.<sup>6</sup>

### MM model preparation.

Protonation state of titrable residues were decided via visual inspection of hydrogen bonds. The residues glutamine, asparagine and histidine were checked whether they were correctly orientated as in crystal structures it is generally not possible to distinguish between carbon and nitrogen. No arginine and lysine residues were deprotonated, and no glutamate was protonated. The aspartate residues  $\alpha$ -9<sup>Asp</sup>,  $\beta$ -30<sup>Asp</sup> and  $\beta$ -73<sup>Asp</sup> were protonated. As for histidine protonation state in the protein, the following were protonated on the  $\epsilon$  nitrogen:  $\alpha$ -18<sup>His</sup>,  $\alpha$ -70<sup>His</sup>,  $\alpha$ -81<sup>His</sup>,  $\alpha$ -91<sup>His</sup>,  $\alpha$ -106<sup>His</sup>,  $\alpha$ -120<sup>His</sup>,  $\alpha$ -180<sup>His</sup>,  $\alpha$ -181<sup>His</sup>,  $\alpha$ -234<sup>His</sup>,  $\alpha$ -248<sup>His</sup>,  $\alpha$ -342<sup>His</sup>,  $\alpha$ -416<sup>His</sup>,  $\alpha$ -423<sup>His</sup>,  $\alpha$ -426<sup>His</sup>,  $\alpha$ -453<sup>His</sup>,  $\beta$ -51<sup>His</sup>,  $\beta$ -67<sup>His</sup>,  $\beta$ -158<sup>His</sup>,  $\beta$ -234<sup>His</sup>,  $\beta$ -321<sup>His</sup>,  $\beta$ -379<sup>His</sup>,  $\beta$ -409<sup>His</sup>,  $\beta$ -461<sup>His</sup> and  $\gamma$ -111<sup>His</sup>. The following histidine residues were protonated on the  $\delta$  nitrogen:  $\alpha$ -364<sup>His</sup>,  $\alpha$ -448<sup>His</sup>,  $\beta$ -80<sup>His</sup>,  $\beta$ -177<sup>His</sup>,  $\beta$ -334<sup>His</sup>,  $\beta$ -386<sup>His</sup>,  $\beta$ -80<sup>His</sup>,  $\gamma$ -5<sup>His</sup> and  $\gamma$ -110<sup>His</sup>. Only  $\beta$ -150<sup>His</sup> is found to be doubly. Cysteine residues ligated to metals were modeled as deprotonated

cysteinate residues:  $\alpha$ -49<sup>Cys</sup>,  $\alpha$ -138<sup>Cys</sup>,  $\alpha$ -75<sup>Cys</sup>,  $\alpha$ -257<sup>Cys</sup>,  $\beta$ -31<sup>His</sup>,  $\beta$ -56<sup>Cys</sup> and  $\beta$ -115<sup>His</sup>. The following residues had their functional group flipped:  $\alpha$ -120<sup>His</sup>,  $\alpha$ -249<sup>Gln</sup>,  $\alpha$ -426<sup>His</sup>,  $\beta$ -243<sup>His</sup>,  $\beta$ -260<sup>Asn</sup>,  $\beta$ -267<sup>Gln</sup>,  $\beta$ -361<sup>Gln</sup>,  $\gamma$ -3<sup>Gln</sup> and  $\gamma$ -46<sup>Gln</sup>

The total charge of the system after protonation by GROMACS is -62 and 62 sodium ions were generated in the solute (by randomly replacing water molecules) to neutralize the charge. The size of the periodic box is 174.97 \* 174.97 \* 174.97 Å with all angles set at 90°. The total volume of the system after solvation is 5356.17 nm<sup>3</sup> and has a density of 1006.33 g/l. The final MM model size is 531 080 atoms.

### MD simulations

All hydrogen atoms, water molecules and sodium ions of the system were then relaxed (all other atoms were kept constrained) using the steepest descent algorithm. The MM model was simulated within the canonical ensemble, with the same constraints, using the velocity-Verlet algorithm<sup>7,8</sup> and coupled to a 4-chain Nosé-Hoover thermostat<sup>9-12</sup>. The system was heated up from 50 K to 300 K in 500 ps and maintained at 300 K for a total of 5 ns. At 1100 ps a snapshot was extracted.

### QM/MM preparation and calculations.

A spherical cut-out cluster model was generated from a snapshot from the MD trajectory after 1100 ps (Figure 2 in article). All residues, as labelled in the 5N6Y X-ray structure,<sup>13</sup> from chain A (residues numbered 2 to 474), chain B (residues numbered 12 to 475), chain C (residues numbered from 2 to 113) and chain E (residues numbered 12 to 475) and water molecules within 42 Å of the carbide of FeVco are included. 35 sodium ions are included as well to keep the system charge neutral. In total, we are including all residues from  $\alpha\beta\gamma$  subunits. The QM/MM model contains 32 562 atoms. An active region of 1038 atoms was used in all QM/MM optimizations except in separate calculations concerning the protonation state of FeVco. As the carboxylate arm of homocitrate reaches the boundary of the defined active region, the active region size was increased to include all residues within 13 Å of the central carbide (as compared to 10 Å for previous calculations) to accommodate for the area around the carboxylate group. All protonated models utilize this active region size. Three different QM regions were used: 57, 83 and 181 atoms, shown in Figure S2-S4.

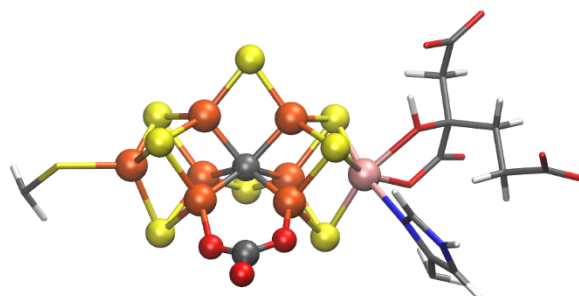


Figure S1: 57 QM atom region, [VFe<sub>7</sub>S<sub>8</sub>CXO<sub>3</sub>], homocitrate, Cys<sup>257</sup> and His<sup>423</sup>.

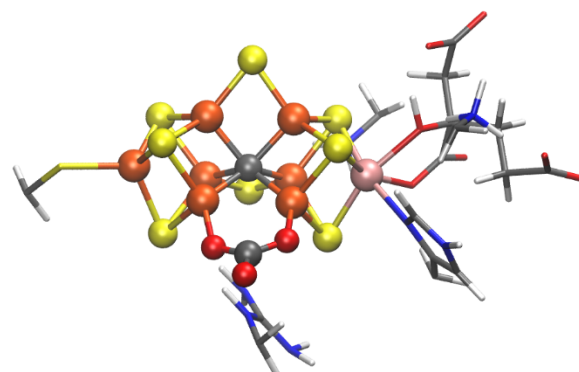


Figure S2: 83 QM atom region, [VFe<sub>7</sub>S<sub>8</sub>CXO<sub>3</sub>], homocitrate, Cys<sup>257</sup>, His<sup>423</sup>, Arg<sup>339</sup>, Lys<sup>83</sup> and Lys<sup>361</sup>.

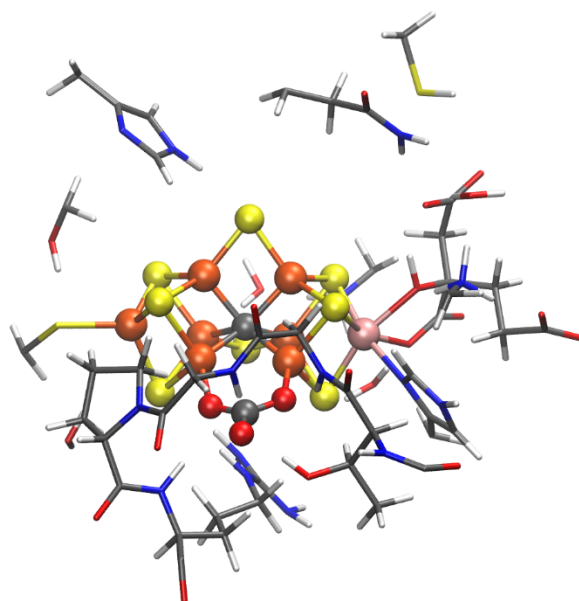


Figure S 3: 181 QM atom region,  $[VFe_7S_8CXO_3]$ , homocitrate, Cys<sup>257</sup>, His<sup>423</sup>, Arg<sup>339\*</sup>, Lys<sup>83</sup>, Lys<sup>361</sup>, Ser<sup>260</sup>, His<sup>180</sup>, Gln<sup>176</sup>, Cys<sup>52</sup>, Thr<sup>335</sup>, Gly<sup>336</sup>, Gly<sup>337</sup> and Pro<sup>338</sup> (\* the QM size of Arg<sup>339</sup> has been increased to include also the whole sidechain and the peptide backbone). Few water molecules have been included as well.

## References

- (1) Best, R. B.; Zhu, X.; Shim, J.; Lopes, P. E. M.; Mittal, J.; Feig, M.; MacKerell, A. D. Optimization of the Additive CHARMM All-Atom Protein Force Field Targeting Improved Sampling of the Backbone Phi, Psi and Side-Chain Chi(1) and Chi(2) Dihedral Angles. *J. Chem. Theory Comput.* **2012**, *8* (9), 3257–3273. <https://doi.org/DOI.10.1021/ct3004000x>.
- (2) Klamt, A.; Schüürmann, G. COSMO: A New Approach to Dielectric Screening in Solvents with Explicit Expressions for the Screening Energy and Its Gradient. *J. Chem. Soc., Perkin Trans. 2* **1993**, No. 5, 799–805. <https://doi.org/10.1039/P29930000799>.
- (3) Benediktsson, B.; Bjornsson, R. QM/MM Study of the Nitrogenase MoFe Protein Resting State: Broken-Symmetry States, Protonation States, and QM Region Convergence in the FeMoco Active Site. *Inorg. Chem.* **2017**, *56* (21), 13417–13429. <https://doi.org/10.1021/acs.inorgchem.7b02158>.
- (4) Chang, C. H.; Kim, K. Density Functional Theory Calculation of Bonding and Charge Parameters for Molecular Dynamics Studies on [FeFe] Hydrogenases. *J. Chem. Theory Comput.* **2009**, *5* (4), 1137–1145. <https://doi.org/10.1021/ct800342w>.
- (5) Wright, L. B.; Rodger, P. M.; Walsh, T. R. Aqueous Citrate: A First-Principles and Force-Field Molecular Dynamics Study. *RSC Adv.* **2013**, *3* (37), 16399. <https://doi.org/10.1039/c3ra42437e>.
- (6) Jorgensen, W. L.; Chandrasekhar, J.; Madura, J. D.; Impey, R. W.; Klein, M. L. Comparison of Simple Potential Functions for Simulating Liquid Water. *J. Chem. Phys.* **1983**, *79* (2), 926–935. <https://doi.org/10.1063/1.445869>.
- (7) Swope, W. C.; Andersen, H. C.; Berens, P. H.; Wilson, K. R. A Computer Simulation Method for the Calculation of Equilibrium Constants for the Formation of Physical Clusters of Molecules: Application to Small Water Clusters. *J. Chem. Phys.* **1982**, *76* (1), 637–649. <https://doi.org/10.1063/1.442716>.

- (8) Verlet, L. Computer “Experiments” on Classical Fluids. I. Thermodynamic Properties of Lennard-Jones Molecules. *Phys. Rev.* **1967**, *159* (1), 98–103.
- (9) Nosé, S. A Unified Formulation of the Constant Temperature Molecular Dynamics Methods. *J. Chem. Phys.* **1984**, *81* (1), 511–519. <https://doi.org/10.1063/1.447334>.
- (10) Nosé, S. A Molecular Dynamics Method for Simulations in the Canonical Ensemble. *Mol. Phys.* **1984**, *52* (2), 255–268. <https://doi.org/10.1080/00268978400101201>.
- (11) Hoover, W. G. Canonical Dynamics: Equilibrium Phase-Space Distributions. *Phys Rev A* **1985**, *31* (3), 1695–1697. <https://doi.org/10.1103/PhysRevA.31.1695>.
- (12) Martyna, G. J.; Klein, M. L.; Tuckerman, M. Nosé-Hoover Chains: The Canonical Ensemble via Continuous Dynamics. *J. Chem. Phys.* **1992**, *97* (4), 2635–2643. <https://doi.org/10.1063/1.463940>.
- (13) Sippel, D.; Einsle, O. The Structure of Vanadium Nitrogenase Reveals an Unusual Bridging Ligand. *Nat. Chem. Biol.* **2017**, *13* (9), 956–960. <https://doi.org/10.1038/nchembio.2428>.

## Single Point Broken Symmetry Solution Comparison

We calculated 35 BS solutions for multiple combinations of ligand ( $\text{CO}_3$ ,  $\text{NO}_3$ ), redox state and spin state using the X-ray structure. Relative energies of the BS solutions are shown in Figures S5-S18 and Table S1 for each model. Energies are always relative the most stable BS7-235 solution for each model.

Figure S19 shows a BS-state comparison of different density functionals for the  $[\text{V-CO}_3]^{2-}$  model and Figure S20 compares QM/MM vs. CPCM results.

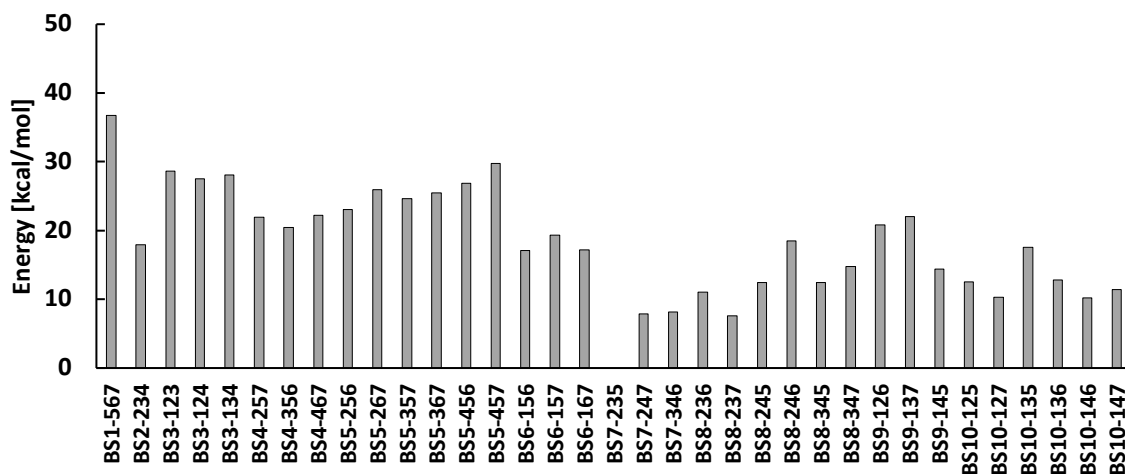


Figure S 4: The relative energies of the 35 BS solutions for  $[\text{V-CO}_3]^{2-}$  and  $M_S = 3/2$ . Functional: TPSSh. QM-region size: 57 atoms. Energies are relative to the  $M_S = 3/2$  BS7-235 solution.

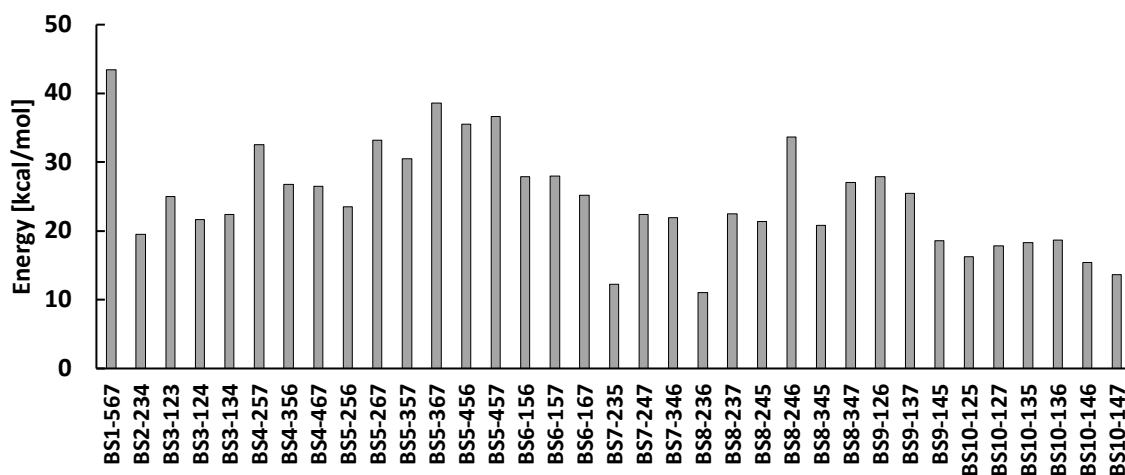


Figure S 5: The relative energies of the 35 BS solutions for  $[\text{V-CO}_3]^{2-}$  and  $M_S = 1/2$ . Functional: TPSSh. QM-region size: 57 atoms. Energies are relative to the  $M_S = 3/2$  BS7-235 solution.

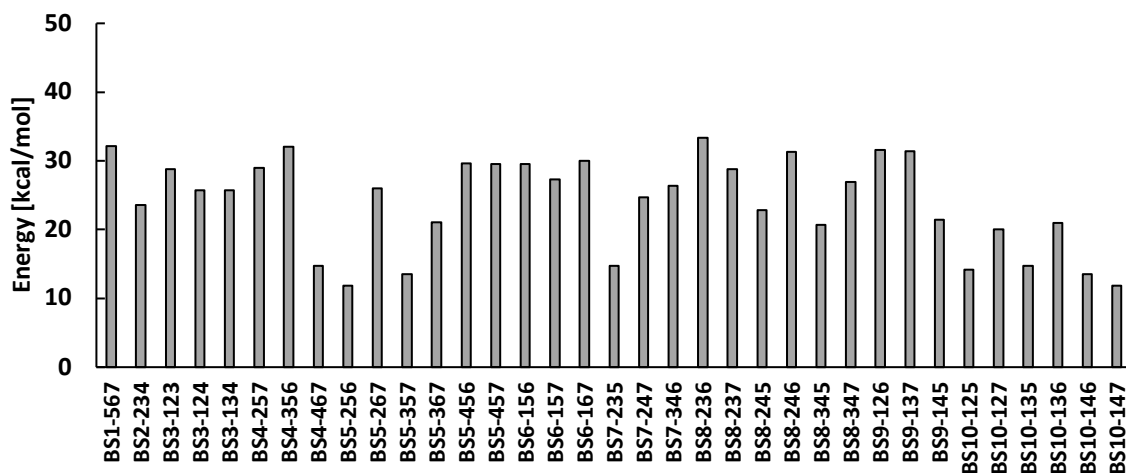


Figure S 6: The relative energies of the 35 BS solutions for  $[V-CO_3]^-$  and  $M_S = 0$ . Functional: TPSSh. QM-region size: 57 atoms. Energies are relative to the  $M_S = 1$  BS7-235 solution.

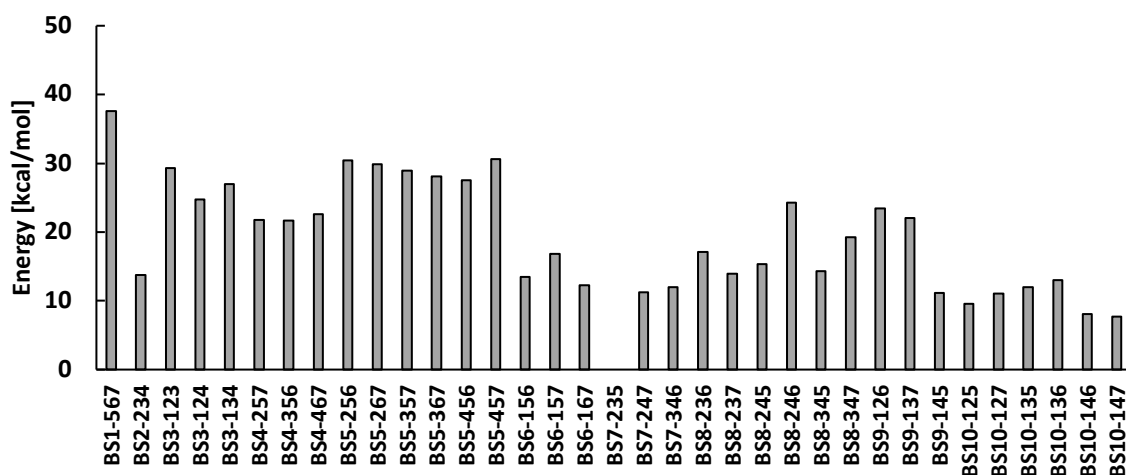


Figure S 7: The relative energies of the 35 BS solutions for  $[V-CO_3]^-$  and  $M_S = 1$ . Functional: TPSSh. QM-region size: 57 atoms. Energies are relative to the  $M_S = 1$  BS7-235 solution.

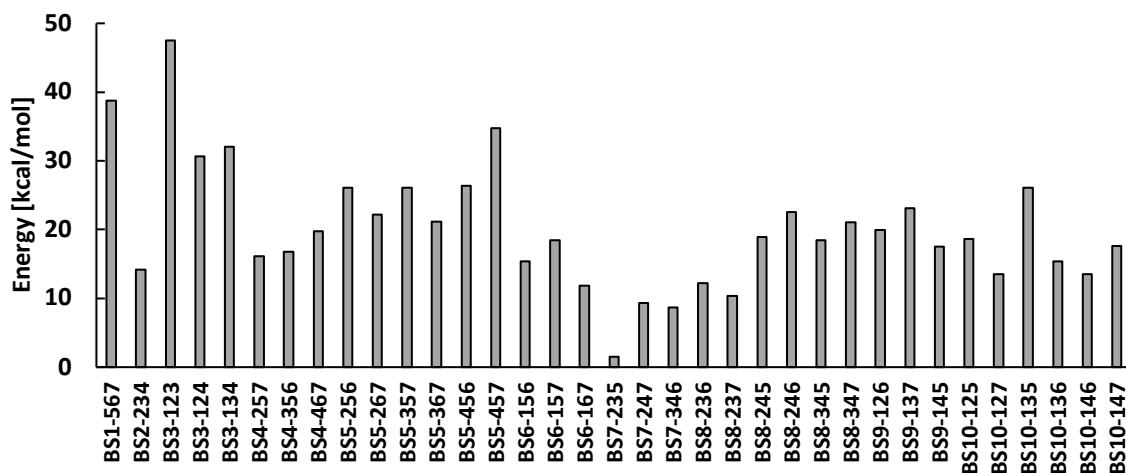


Figure S 8: The relative energies of the 35 BS solutions for  $[V-CO_3]^0$  and  $M_S = 2$ . Functional: TPSSh. QM-region size: 57 atoms. Energies are relative to the  $M_S = 1$  BS7-235 solution.

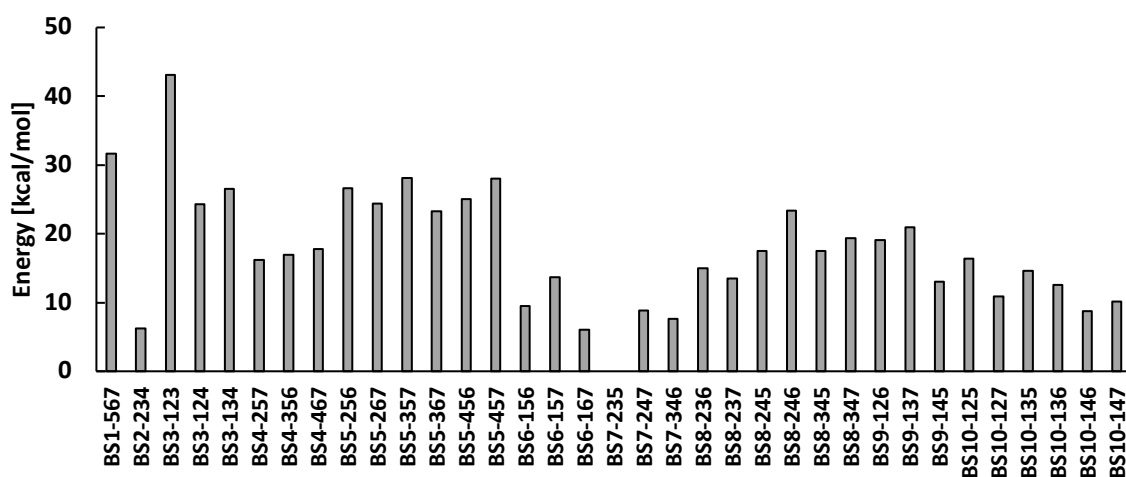


Figure S 9: The relative energies of the 35 BS solutions for  $[V-CO_3]^0$  and  $M_S = 3/2$ . Functional: TPSSh. QM-region size: 57 atoms. Energies are relative to the  $M_S = 3/2$  BS7-235 solution.

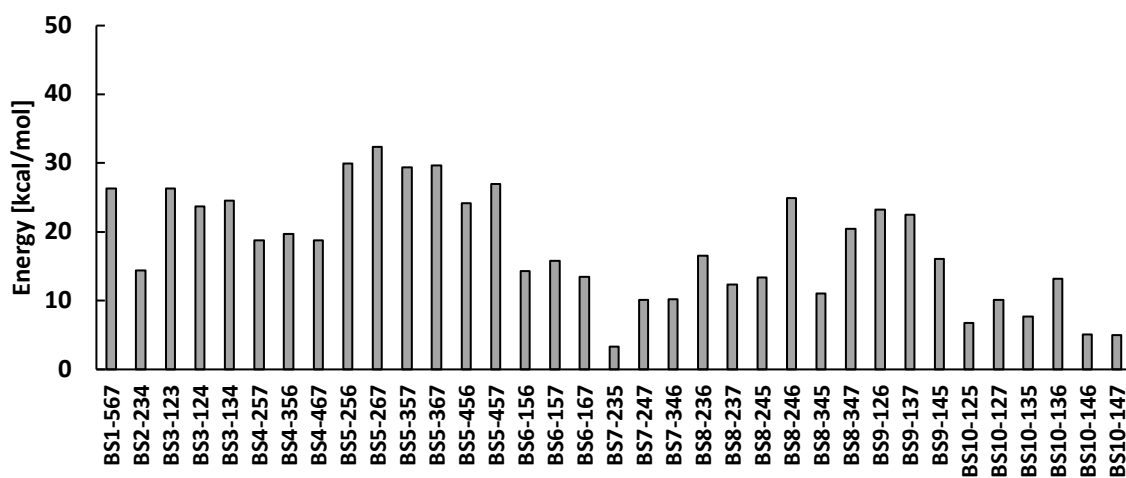


Figure S 10: The relative energies of the 35 BS solutions for  $[V-CO_3]^0$  and  $M_S = 1/2$ . Functional: TPSSh. QM-region size: 57 atoms. Energies are relative to the  $M_S = 3/2$  BS7-235 solution.

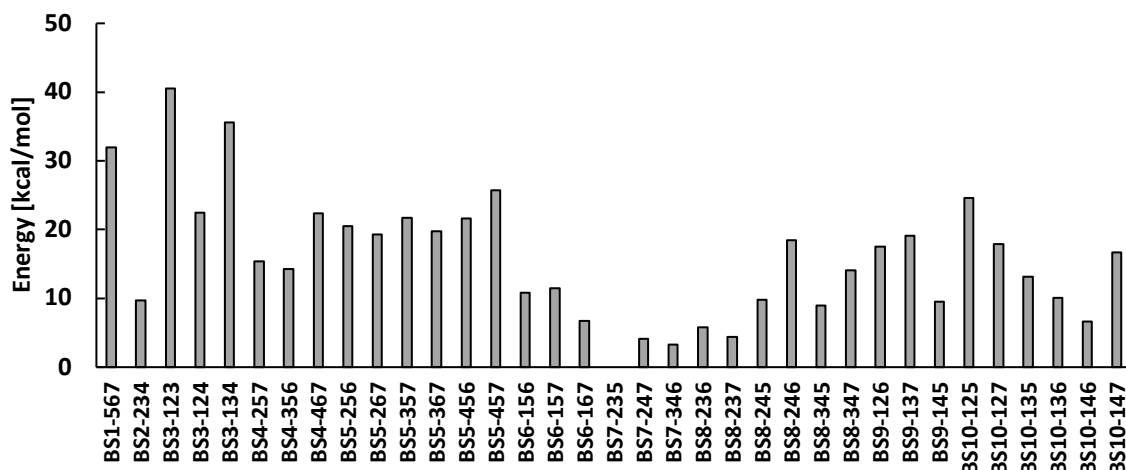


Figure S 11: The relative energies of the 35 BS solutions for  $[V-NO_3]^-$  and  $M_S = 3/2$ . Functional: TPSSh. QM-region size: 57 atoms. Energies are relative to the  $M_S = 3/2$  BS7-235 solution.

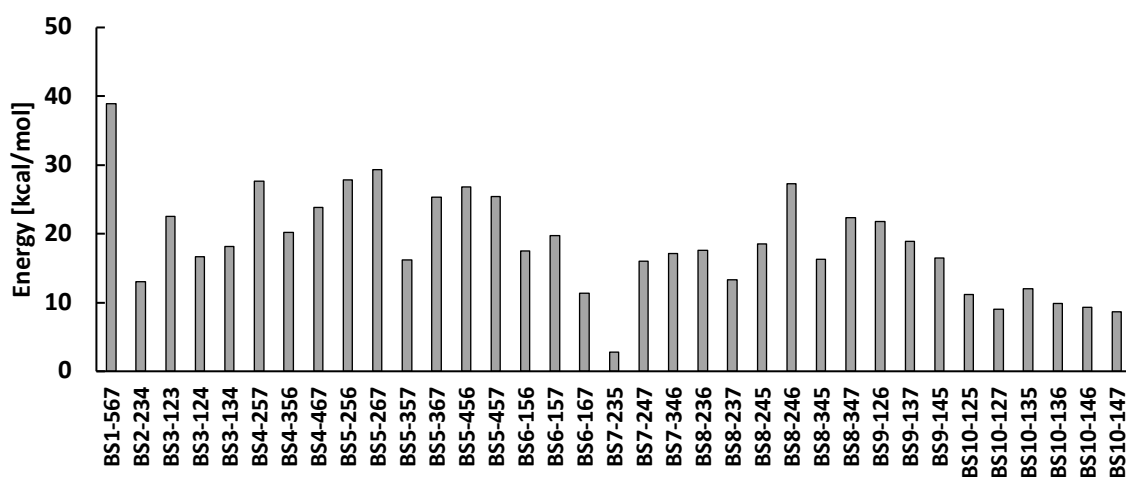


Figure S 12: Figure S 13: The relative energies of the 35 BS solutions for  $[V-NO_3]^-$  and  $M_S = 1/2$ . Functional: TPSSh. QM-region size: 57 atoms. Energies are relative to the  $M_S = 3/2$  BS7-235 solution.

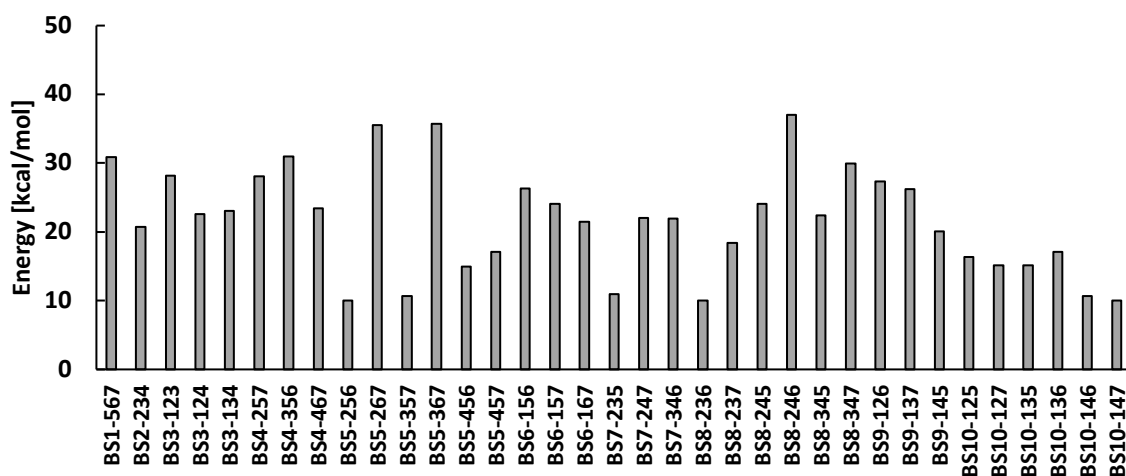


Figure S 14: The relative energies of the 35 BS solutions for  $[V-NO_3]^0$  and  $M_S = 0$ . Functional: TPSSh. QM-region size: 57 atoms. Energies are relative to the  $M_S = 1$  BS7-235 solution.



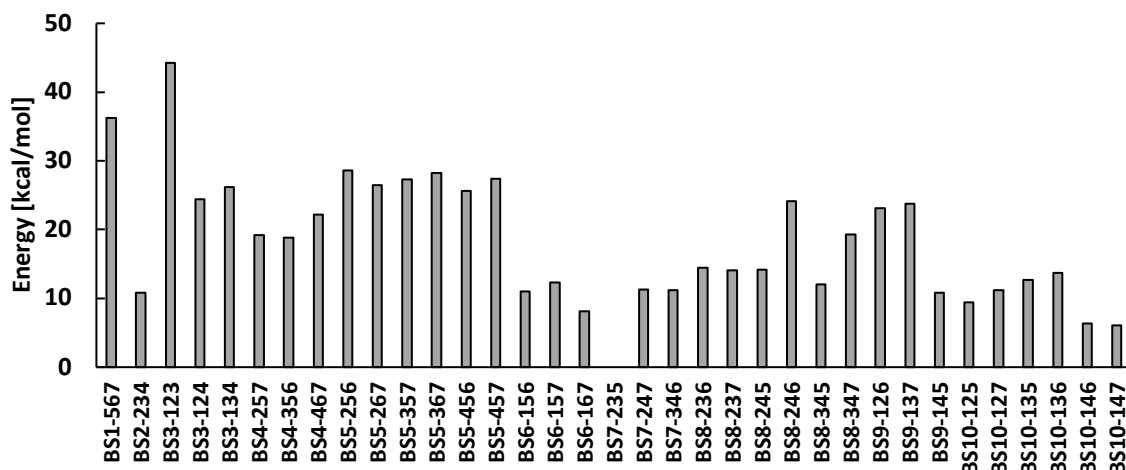


Figure S 15: The relative energies of the 35 BS solutions for  $[V-NO_3]^0$  and  $M_S = 1$ . Functional: TPSSh. QM-region size: 57 atoms. Energies are relative to the  $M_S = 1$  BS7-235 solution.

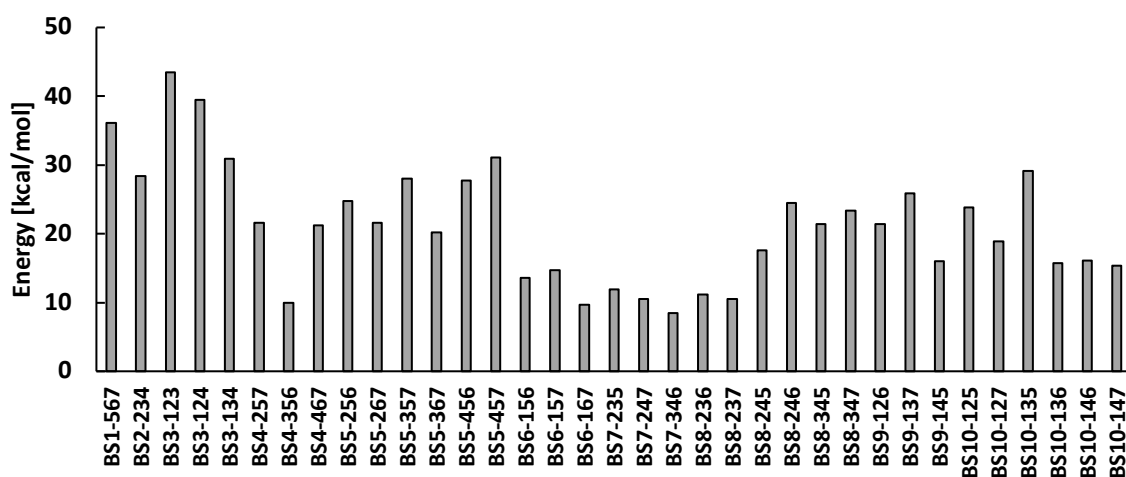


Figure S 16: The relative energies of the 35 BS solutions for  $[V-NO_3]^0$  and  $M_S = 1$ . Functional: TPSSh. QM-region size: 57 atoms. Energies are relative to the  $M_S = 1$  BS7-235 solution.

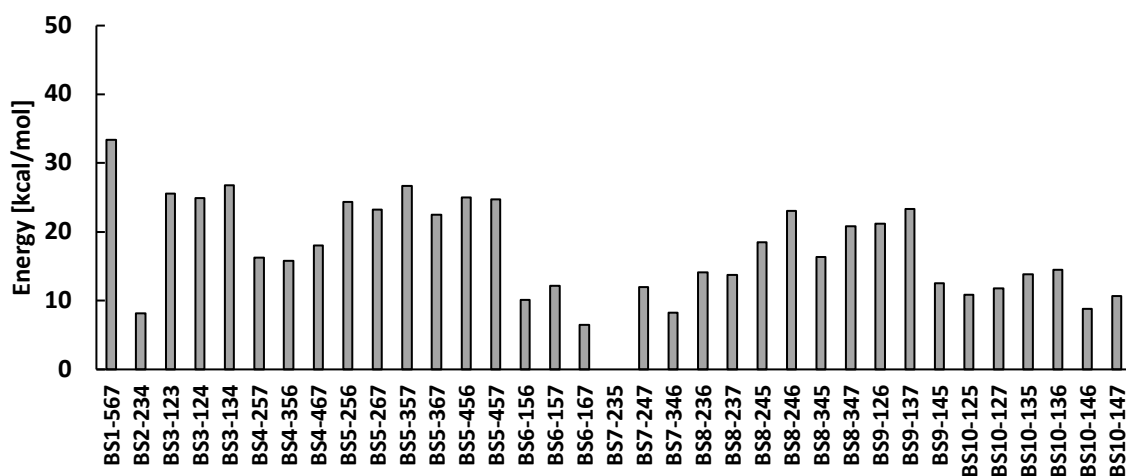


Figure S 17: The relative energies of the 35 BS solutions for  $[V-NO_3]^+$  and  $M_S = 3/2$ . Functional: TPSSh. QM-region size: 57 atoms. Energies are relative to the  $M_S = 3/2$  BS7-235 solution.

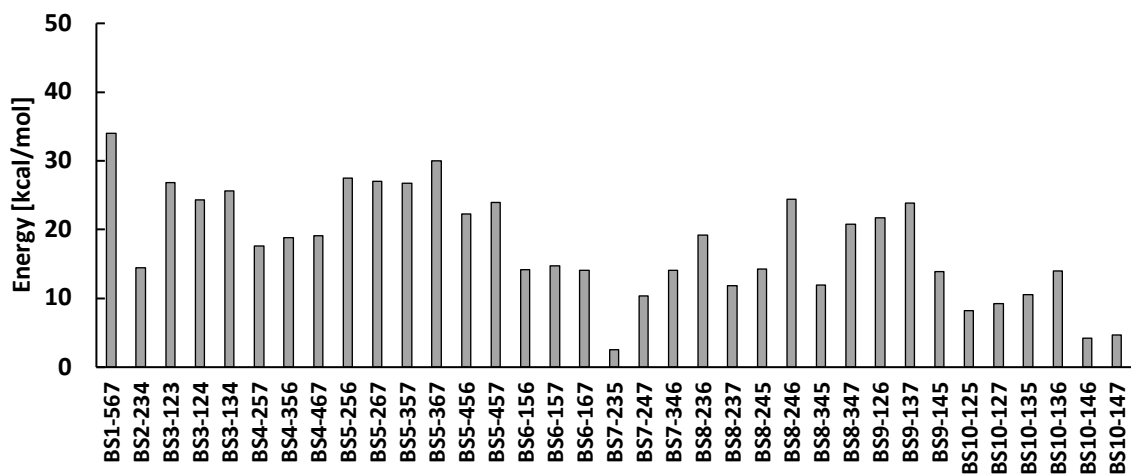


Figure S 18: The relative energies of the 35 BS solutions for  $[V-NO_3]^+$  and  $M_S = 1/2$ . Functional: TPSSh. QM-region size: 57 atoms. Energies are relative to the  $M_S = 3/2$  BS7-235 solution.

Table S 1: Relative QM/MM energies (kcal/mol) of all BS solutions for all FeVco models using the crystal structure geometry. The \* indicates the high-spin energy relative to the preferred BS solution. ( $M_S = 3/2$  for  $[V-CO_3]^{2-}$  and  $[V-NO_3]^-$ ,  $M_S = 3/2$  for  $[V-CO_3]^-$  and  $[V-NO_3]^0$ , and  $M_S = 3/2$  for  $[V-CO_3]^0$  and  $[V-NO_3]^+$ ).

	Carbonate							Nitrate						
	$[V-CO_3]^{2-}$ $M_S = 3/2$	$[V-CO_3]^{2-}$ $M_S = 1/2$	$[V-CO_3]^-$ $M_S = 0$	$[V-CO_3]^-$ $M_S = 1$	$[V-CO_3]^-$ $M_S = 2$	$[V-CO_3]^0$ $M_S = 3/2$	$[V-CO_3]^0$ $M_S = 1/2$	$[V-NO_3]^-$ $M_S = 3/2$	$[V-NO_3]^-$ $M_S = 1/2$	$[V-NO_3]^0$ $M_S = 0$	$[V-NO_3]^0$ $M_S = 1$	$[V-NO_3]^0$ $M_S = 2$	$[V-NO_3]^+$ $M_S = 3/2$	$[V-NO_3]^+$ $M_S = 1/2$
BS1-567	36.77	43.47	32.16	37.57	38.74	31.68	26.30	31.94	38.92	30.83	36.20	36.10	33.37	34.00
BS2-234	17.90	19.47	23.62	13.75	14.15	6.19	14.36	9.71	13.06	20.69	10.86	28.37	8.20	14.47
BS3-123	28.68	24.98	28.77	29.26	47.47	43.10	26.35	40.52	22.56	28.22	44.29	43.47	25.60	26.82
BS3-124	27.49	21.62	25.70	24.69	30.64	24.29	23.67	22.48	16.63	22.62	24.42	39.49	24.92	24.31
BS3-134	28.12	22.37	25.76	26.94	32.06	26.52	24.57	35.55	18.14	23.02	26.21	30.95	26.75	25.60
BS4-257	21.91	32.56	28.98	21.72	16.18	16.20	18.75	15.41	27.64	28.10	19.21	21.60	16.30	17.66
BS4-356	20.40	26.75	32.01	21.69	16.74	16.90	19.70	14.23	20.18	30.94	18.85	9.99	15.79	18.81
BS4-467	22.18	26.52	14.75	22.64	19.81	17.78	18.74	22.34	23.82	23.42	22.22	21.23	18.05	19.10
BS5-256	23.01	23.54	11.83	30.43	26.10	26.62	29.95	20.51	27.87	9.99	28.57	24.73	24.33	27.50
BS5-267	25.94	33.23	26.04	29.89	22.17	24.43	32.35	19.31	29.36	35.53	26.44	21.55	23.28	27.06
BS5-357	24.60	30.45	13.49	28.97	26.13	28.08	29.34	21.72	16.21	10.68	27.32	28.06	26.69	26.78
BS5-367	25.47	38.61	21.09	28.12	21.15	23.29	29.63	19.76	25.28	35.69	28.24	20.17	22.51	30.03
BS5-456	26.86	35.49	29.62	27.57	26.33	25.05	24.16	21.64	26.78	14.99	25.66	27.72	24.98	22.30
BS5-457	29.78	36.61	29.51	30.65	34.77	27.98	26.93	25.68	25.44	17.14	27.42	31.07	24.78	23.98
BS6-156	17.12	27.90	29.55	13.49	15.38	9.47	14.32	10.81	17.54	26.35	11.04	13.63	10.11	14.15
BS6-157	19.30	27.99	27.32	16.87	18.42	13.70	15.80	11.50	19.76	24.03	12.30	14.74	12.19	14.75
BS6-167	17.16	25.21	30.00	12.27	11.83	6.09	13.45	6.72	11.34	21.43	8.10	9.67	6.50	14.06
BS7-235	0.00	12.29	14.75	0.00	1.51	0.00	3.27	0.00	2.76	10.90	0.00	11.95	0.00	2.51
BS7-247	7.83	22.41	24.67	11.20	9.37	8.84	10.09	4.09	15.97	22.03	11.27	10.49	11.94	10.38
BS7-346	8.18	21.98	26.40	11.99	8.67	7.63	10.16	3.30	17.13	21.90	11.24	8.42	8.25	14.13
BS8-236	11.08	11.08	33.39	17.10	12.24	15.02	16.51	5.77	17.63	9.99	14.46	11.16	14.11	19.19
BS8-237	7.58	22.47	28.79	13.95	10.32	13.52	12.31	4.41	13.27	18.42	14.05	10.55	13.74	11.86
BS8-245	12.42	21.39	22.79	15.33	18.92	17.51	13.38	9.77	18.52	24.07	14.13	17.62	18.51	14.24
BS8-246	18.52	33.68	31.33	24.29	22.59	23.40	24.90	18.46	27.25	37.00	24.13	24.46	23.02	24.44
BS8-345	12.48	20.86	20.74	14.27	18.47	17.46	11.01	8.92	16.29	22.41	12.08	21.44	16.39	11.97
BS8-347	14.77	27.08	26.96	19.29	21.03	19.32	20.40	14.09	22.33	29.98	19.29	23.33	20.80	20.75
BS9-126	20.77	27.93	31.55	23.41	19.91	19.12	23.24	17.50	21.80	27.36	23.09	21.41	21.16	21.74
BS9-137	22.00	25.48	31.42	22.06	23.16	20.98	22.52	19.09	18.92	26.23	23.72	25.84	23.34	23.91
BS9-145	14.40	18.56	21.41	11.16	17.53	13.04	16.05	9.52	16.51	20.06	10.85	16.04	12.50	13.88
BS10-125	12.56	16.21	14.20	9.60	18.64	16.38	6.74	24.61	11.18	16.38	9.45	23.81	10.86	8.24
BS10-127	10.28	17.80	20.04	11.06	13.56	10.84	10.12	17.93	9.02	15.16	11.17	18.93	11.77	9.22
BS10-135	17.56	18.32	14.71	12.02	26.06	14.63	7.66	13.20	12.02	15.10	12.69	29.17	13.85	10.53
BS10-136	12.79	18.64	20.94	12.98	15.42	12.59	13.22	10.09	9.85	17.14	13.67	15.69	14.51	13.98
BS10-146	10.18	15.44	13.49	8.12	13.53	8.75	5.06	6.64	9.32	10.68	6.38	16.10	8.84	4.22
BS10-147	11.38	13.64	11.83	7.73	17.65	10.18	4.95	16.70	8.68	9.99	6.10	15.39	10.63	4.70
Hi-Spin*	132.53			149.53		160.57		128.07			147.79		162.17	

Table S 2: Relative QM/MM energies (kcal/mol) of different spin-flip procedures for  $[V-CO_3]^{2-}$ , where the spin of V is either flipped after the BS solution is converged or the spin of V is flipped along with the spins of the irons from the high spin solution.. All energies are relative to the BS7-235 solution of the 'normal flip spin' column (which is the same as BS7-235 in the first column,  $[V-CO_3]^{2-}$  and  $M_S = 3/2$  in Table S1).

	Normal flip spin <sup>a</sup>	V-flip from low spin <sup>b</sup>	V-flip from high spin <sup>c</sup>	Difference between 'V-flip from low spin' and 'normal flip spin'	Difference between 'V-flip from high spin' and 'normal flip spin'
BS1-567	36.77	36.77	36.77	0.00	0.00
BS2-234	17.90	17.85	16.48	-0.05	-1.41
BS3-123	28.68	28.68	28.68	0.00	0.00
BS3-124	27.49	27.48	29.05	0.00	1.57
BS3-134	28.12	28.12	28.12	0.00	0.00
BS4-257	21.91	21.91	21.91	0.00	0.00
BS4-356	20.40	20.40	20.40	0.00	0.00
BS4-467	22.18	22.18	22.18	0.00	0.00
BS5-256	23.01	23.01	23.01	0.00	0.00
BS5-267	25.94	25.94	25.94	0.00	0.00
BS5-357	24.60	24.60	24.60	0.00	0.00
BS5-367	25.47	25.47	25.47	0.00	0.00
BS5-456	26.86	26.86	26.86	0.00	0.00
BS5-457	29.78	29.78	29.71	0.00	-0.07
BS6-156	17.12	17.12	17.12	0.00	0.00
BS6-157	19.30	19.30	19.30	0.00	0.00
BS6-167	17.16	17.16	17.16	0.00	0.00
BS7-235	0.00	0.00	0.00	0.00	0.00
BS7-247	7.83	7.83	7.83	0.00	0.00
BS7-346	8.18	8.18	8.18	0.00	0.00
BS8-236	11.08	11.08	11.08	0.00	0.00
BS8-237	7.58	7.58	7.58	0.00	0.00
BS8-245	12.42	12.42	12.42	0.00	0.00
BS8-246	18.52	18.52	18.52	0.00	0.00
BS8-345	12.48	12.48	12.48	0.00	0.00
BS8-347	14.77	14.77	14.77	0.00	0.00
BS9-126	20.77	20.77	20.77	0.00	0.00
BS9-137	22.00	22.00	22.00	0.00	0.00
BS9-145	14.40	14.40	14.40	0.00	0.00
BS10-125	12.56	12.56	12.56	0.00	0.00
BS10-127	10.28	10.28	10.28	0.00	0.00
BS10-135	17.56	17.56	17.56	0.00	0.00
BS10-136	12.79	12.79	12.79	0.00	0.00
BS10-146	10.18	10.18	10.18	0.00	0.00
BS10-147	11.38	11.38	11.38	0.00	0.00

a) Normal flip spin is the same BS solution as acquired with no specific flipping of vanadium

b) V-flip from low spin means that a fully converged BS solution is used as a "high spin" solution and then vanadium is flipped

c) V-flip from high spin means that first a high spin solution is converged and then in the BS step, the vanadium is included in the flip spin procedure.

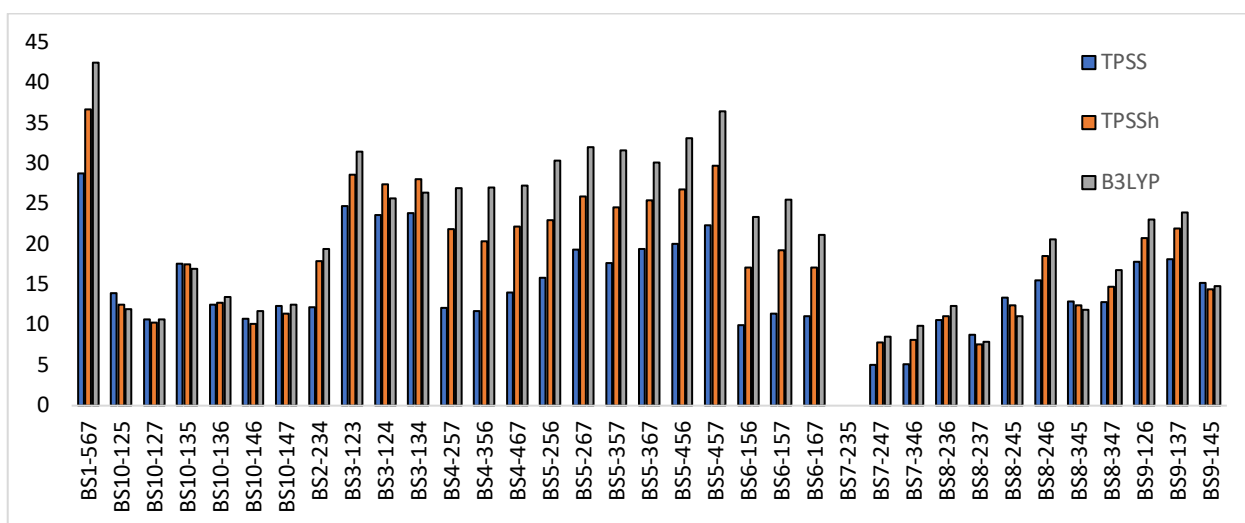


Figure S 19: Relative QM/MM energies of the 35 BS solutions for the  $[V-CO_3]^{2-}$  model using the X-ray structure with different functionals.

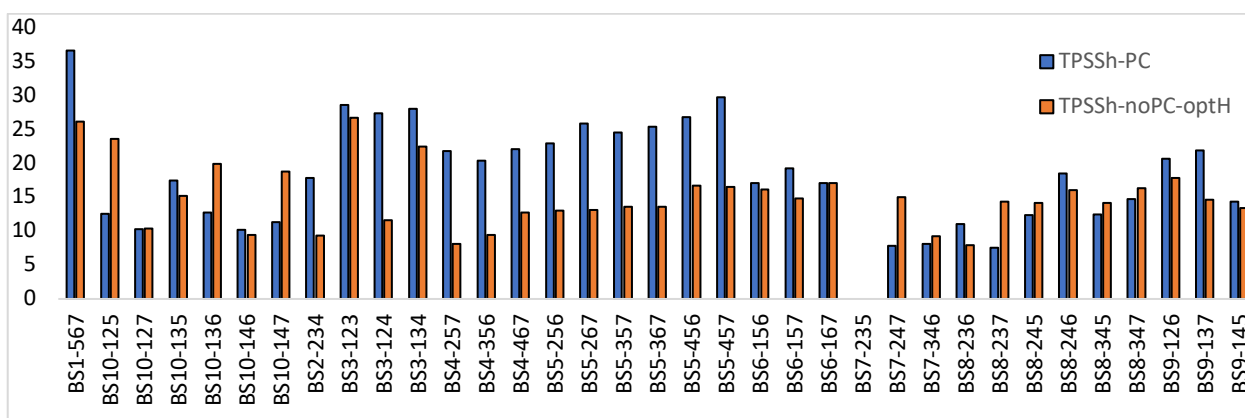


Figure S 20: Comparison of CPCM-DFT energies and QM/MM energies of the 35 BS solutions for the  $[V-CO_3]^{2-}$  model using the X-ray structure. Functional: TPSSh. Homocitrate was calculated as triply protonated.

# Mulliken spin populations of the 181 QM-atom QM/MM optimized structures

Table S 3: Mulliken spin population of the QM/MM optimized models. C\* is carbide and X is either nitrogen or carbon of the XO<sub>3</sub> ligand.

Model Charge Spin QM size	[V-CO <sub>3</sub> ] <sup>n</sup>										[V-NO <sub>3</sub> ] <sup>n</sup>									
	2- 3/2	1- 2	1- 1	1- 0	0 3/2	2- 3/2	1- 2	1- 1	1- 0	0 3/2	1- 3/2	0 2	0 1	0 0	1+ 3/2	1- 3/2	0 2	0 1	0 0	1+ 3/2
	181	181	181	181	181	57	57	57	57	57	181	181	181	181	181	57	57	57	57	57
V	-1.62	1.00	-1.58	-1.59	-1.52	-1.65	1.02	-1.61	-1.61	-0.65	-1.69	-1.66	-1.67	-1.62	-1.56	-1.73	0.85	-1.69	-1.65	-0.84
Fe1	3.45	3.47	3.46	3.37	3.46	3.48	3.49	3.49	2.33	3.49	3.47	3.48	3.48	3.39	3.48	3.50	3.50	3.50	3.43	3.49
Fe2	-3.29	-3.43	-3.44	-3.43	-3.42	-3.29	-3.44	-3.45	-3.49	-3.45	-3.26	-3.17	-3.42	-3.43	-3.40	-3.27	-3.41	-3.42	-3.43	-3.43
Fe3	-3.27	-3.44	-3.45	-3.45	-3.42	-3.29	-3.48	-3.48	-3.47	-3.46	-3.25	-3.17	-3.43	-3.44	-3.39	-3.27	-3.45	-3.45	-3.47	-3.42
Fe4	3.39	3.40	3.40	2.27	3.43	3.43	3.43	3.42	3.26	3.42	3.24	3.29	3.28	2.15	3.32	3.26	3.28	3.28	2.15	3.29
Fe5	-3.19	-3.34	-3.23	-3.27	-3.18	-3.22	-3.37	-3.25	-3.27	-3.30	-3.04	-3.00	-3.09	-3.11	-3.06	-3.06	-3.19	-3.10	-3.13	-3.14
Fe6	3.29	3.29	3.15	3.06	3.39	3.28	3.30	3.18	3.19	3.19	3.27	3.44	3.13	3.05	3.36	3.27	3.28	3.15	3.06	3.17
Fe7	3.21	2.84	3.07	2.97	3.31	3.23	2.88	3.10	3.11	3.18	3.20	3.37	3.06	2.97	3.30	3.22	2.89	3.07	2.97	3.16
S1A	0.20	0.15	0.15	-0.04	0.12	0.18	0.13	0.13	-0.09	0.11	0.20	0.20	0.16	-0.04	0.14	0.18	0.14	0.15	-0.04	0.13
S2A	-0.02	-0.12	-0.13	-0.14	-0.15	-0.02	-0.12	-0.13	-0.32	-0.15	-0.01	-0.05	-0.11	-0.13	-0.14	-0.01	-0.10	-0.11	-0.13	-0.12
S4A	0.17	0.13	0.13	-0.06	0.11	0.16	0.12	0.12	-0.03	0.10	0.18	0.18	0.15	-0.05	0.13	0.18	0.15	0.14	-0.07	0.13
S1B	0.08	0.01	0.09	0.09	0.14	0.09	0.01	0.10	0.10	0.03	0.07	0.11	0.08	0.08	0.11	0.08	0.00	0.08	0.08	0.03
S3B	0.27	0.20	0.28	0.23	0.36	0.27	0.20	0.28	0.28	0.28	0.29	0.37	0.28	0.24	0.36	0.29	0.22	0.29	0.23	0.31
S4B	0.10	-0.06	0.11	0.10	0.14	0.11	-0.06	0.12	0.12	0.06	0.09	0.11	0.09	0.08	0.11	0.09	-0.06	0.09	0.09	0.06
S2B	0.01	-0.07	-0.07	-0.06	0.02	0.02	-0.07	-0.07	-0.08	-0.03	0.01	0.11	-0.07	-0.07	0.01	0.00	-0.08	-0.08	-0.07	-0.04
S5A	0.00	-0.15	-0.10	-0.08	-0.02	0.02	-0.15	-0.09	-0.08	-0.02	0.00	0.08	-0.10	-0.09	-0.02	0.01	-0.14	-0.09	-0.08	-0.03
C*	0.06	-0.07	-0.04	-0.13	0.02	0.06	-0.07	-0.03	-0.03	-0.05	0.06	0.13	-0.03	-0.13	0.03	0.07	-0.06	-0.02	-0.13	-0.04
X	0.00	0.00	0.00	-0.01	0.00	0.00	0.00	0.00	0.00	0.00	0.00	0.00	0.00	-0.02	0.00	0.00	0.01	0.00	-0.02	0.00
O3	0.03	0.04	0.04	0.02	0.05	0.04	0.05	0.05	0.04	0.05	-0.01	-0.01	-0.01	0.01	0.00	-0.01	0.00	0.00	0.01	0.00
O1	-0.01	-0.02	-0.02	-0.02	-0.03	-0.02	-0.04	-0.03	-0.03	-0.05	0.02	0.01	0.01	0.00	0.01	0.01	0.01	0.01	0.00	0.01
O2	0.00	0.00	0.00	-0.01	0.00	0.00	0.00	0.00	0.00	0.00	0.00	0.00	0.00	-0.02	0.00	0.00	0.00	0.00	-0.01	0.00



















## Mayer bond orders for FeMoco and FeVco

Table S 20: Mayer bond order for metal-metal, metal-sulfide and carbide-metal interaction in QM/MM models of FeMoco and FeVco

Cofactor Model QM size	FeVco	FeMoco	FeVco	FeVco	FeMoco
	X-ray <sup>a</sup> 57	X-ray <sup>a</sup> 57	QM/MM 57	QM/MM 181	QM/MM 247
M-Fe5	0.42	0.41	0.38	0.37	0.47
M-Fe6	0.20	0.40	0.16	0.18	0.45
M-Fe7	0.28	0.42	0.27	0.30	0.49
Fe1-Fe2	0.19	0.20	0.20	0.21	0.20
Fe1-Fe3	0.23	0.20	0.22	0.24	0.23
Fe1-Fe4	0.44	0.38	0.42	0.43	0.41
Fe2-Fe3	0.39	0.40	0.40	0.42	0.41
Fe2-Fe4	0.26	0.24	0.23	0.23	0.24
Fe3-Fe4	0.27	0.23	0.23	0.24	0.29
Fe5-Fe6	0.26	0.28	0.24	0.24	0.28
Fe5-Fe7	0.24	0.28	0.21	0.25	0.31
Fe6-Fe7	0.40	0.45	0.40	0.42	0.47
Fe2-Fe6	0.29	0.32	0.28	0.32	0.32
Fe3-Fe7	0.29	0.33	0.28	0.32	0.34
Fe4-Fe5	0.27	0.29	0.29	0.33	0.30
C-Fe2	0.36	0.30	0.36	0.32	0.31
C-Fe3	0.31	0.34	0.37	0.27	0.27
C-Fe4	0.43	0.40	0.48	0.36	0.35
C-Fe5	0.49	0.40	0.50	0.37	0.36
C-Fe6	0.39	0.32	0.38	0.30	0.33
C-Fe7	0.35	0.34	0.33	0.29	0.35
S1A-Fe1	0.68	0.64	0.68	0.69	0.68
S1A-Fe2	0.91	0.77	0.88	0.85	0.86
S1A-Fe4	0.82	0.80	0.82	0.77	0.82
S2A-Fe1	0.90	0.87	0.96	1.00	0.88
S2A-Fe2	0.79	0.76	0.80	0.80	0.77
S2A-Fe3	0.78	0.81	0.80	0.78	0.76
S4A-Fe1	0.65	0.67	0.65	0.73	0.70
S4A-Fe3	0.95	0.85	0.82	0.85	0.93
S4A-Fe4	0.77	0.81	0.74	0.76	0.90
S1B-V	0.86	1.03	0.87	0.81	1.00
S1B-Fe5	0.69	0.75	0.66	0.68	0.71
S1B-Fe6	0.76	0.72	0.76	0.78	0.78
S3B-Fe6	0.69	1.04	0.62	0.71	0.99
S3B-Fe5	0.71	0.66	0.70	0.71	0.67
S3B-Fe7	0.76	0.67	0.84	0.70	0.65
S4B-V	0.89	1.01	0.88	0.84	1.02
S4B-Fe5	0.74	0.71	0.72	0.75	0.75
S4B-Fe7	0.80	0.72	0.82	0.81	0.80
S2B-Fe2	1.04	0.92	1.05	0.99	0.77
S2B-Fe2	1.04	1.10	1.02	1.03	1.04
S5A-Fe3	1.09	1.01	0.99	1.03	0.95
S5A-Fe7	0.97	1.09	1.00	0.96	1.02
S3A-Fe4	N/A	0.94	N/A	N/A	0.70
S3A-Fe5	N/A	0.97	N/A	N/A	0.91
Ave. non bridging Fe-S	0.78	0.75	0.78	0.78	0.78
Ave. bridging Fe-S	1.03	1.01	1.01	1.00	0.90
Average M-S	0.81	1.03	0.79	0.79	1.00

<sup>a</sup> Single point QM/MM using crystal structure geometry with the protein matrix as pointcharges.

## Localized Orbital Analysis of FeVco

The electronic structure of FeVco in redox states  $[V-CO_3]^{2-/-1-/0}$  as interpreted via IAOIBO localized orbital analysis is shown in Figures S21-S23.

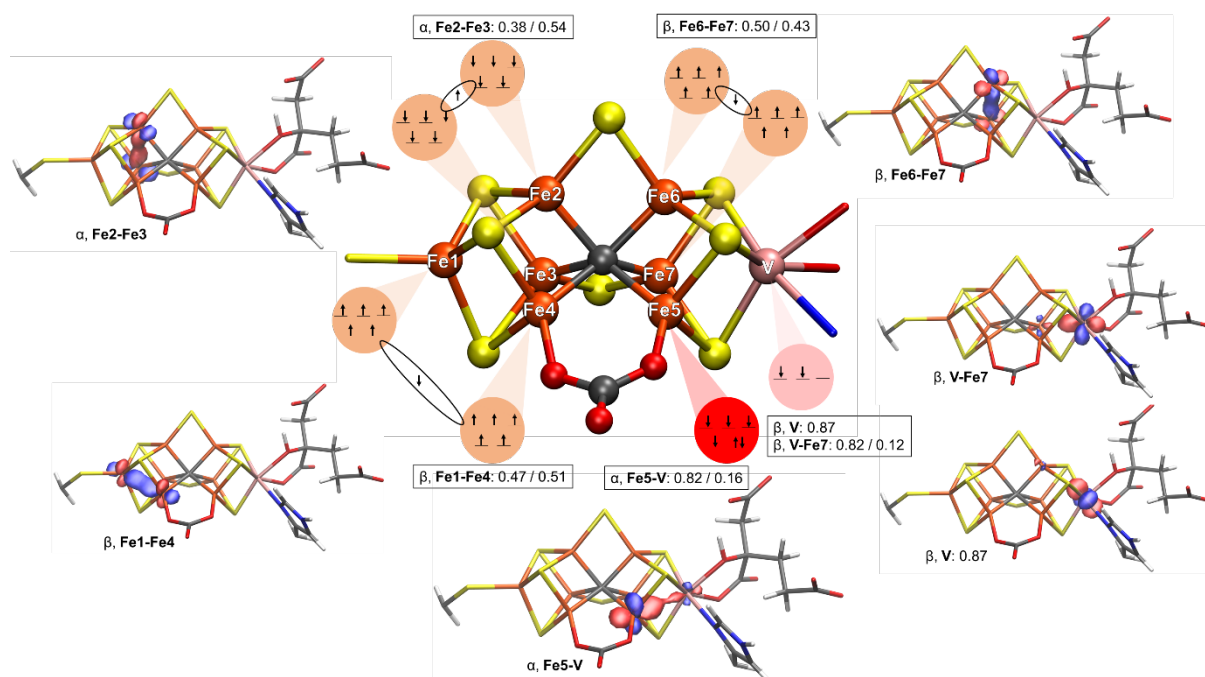


Figure S 21: Electronic structure of  $[V-CO_3]^{2-}$  with  $M_S = 3/2$  as interpreted by IAOIBOs. 181 QM atom QM/MM model. Iso value of 0.1 was used to generate the figures of the orbitals.



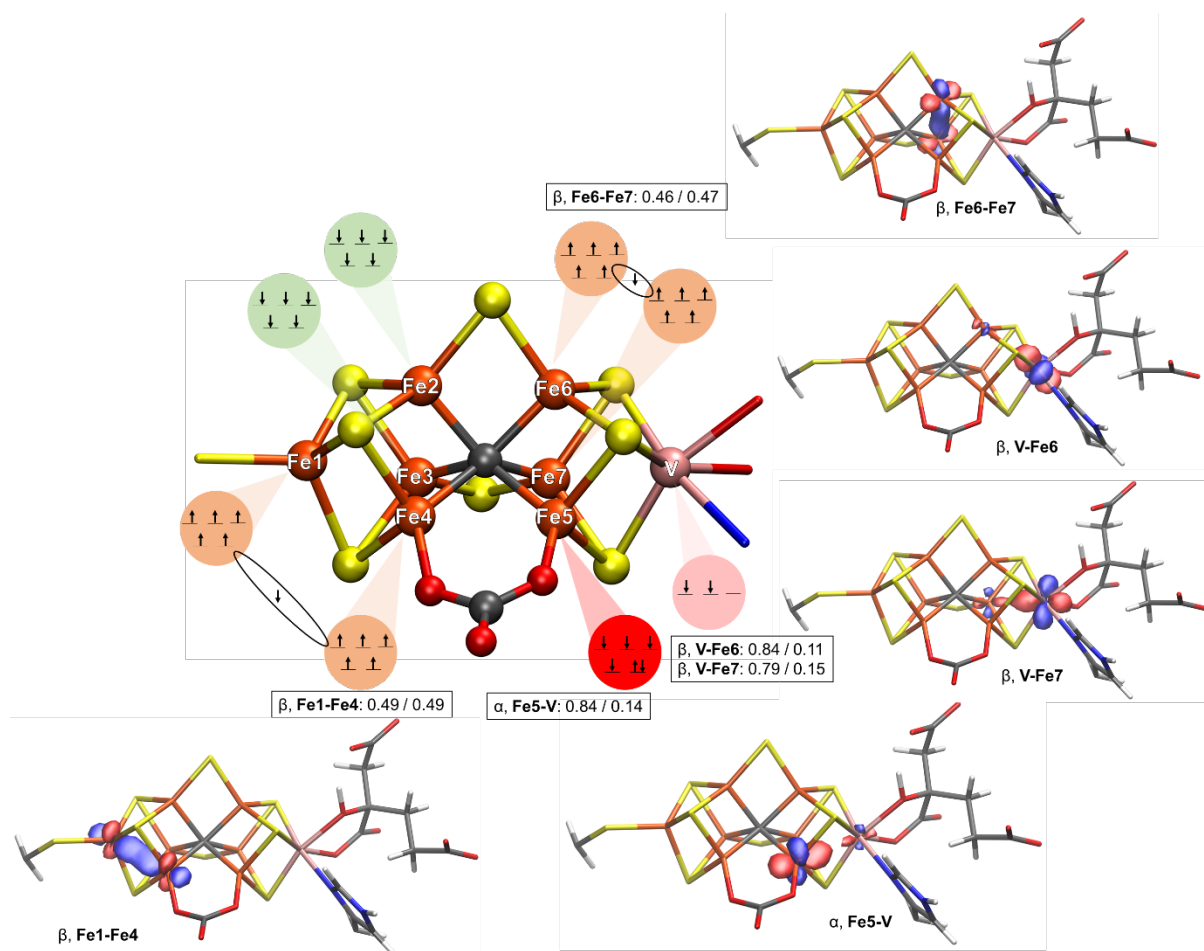


Figure S 22: The electronic structure of  $[V-CO_3]^{1-}$   $M_S = 1$  BS7-235 model as interpreted by LAOIBOs. Shown are localized orbitals for the minority-spin electrons and the vanadium electrons and the atomic populations. Using 181 QM atom QM/MM model. Iso value of 0.1 was used to generate the figures of the orbitals.

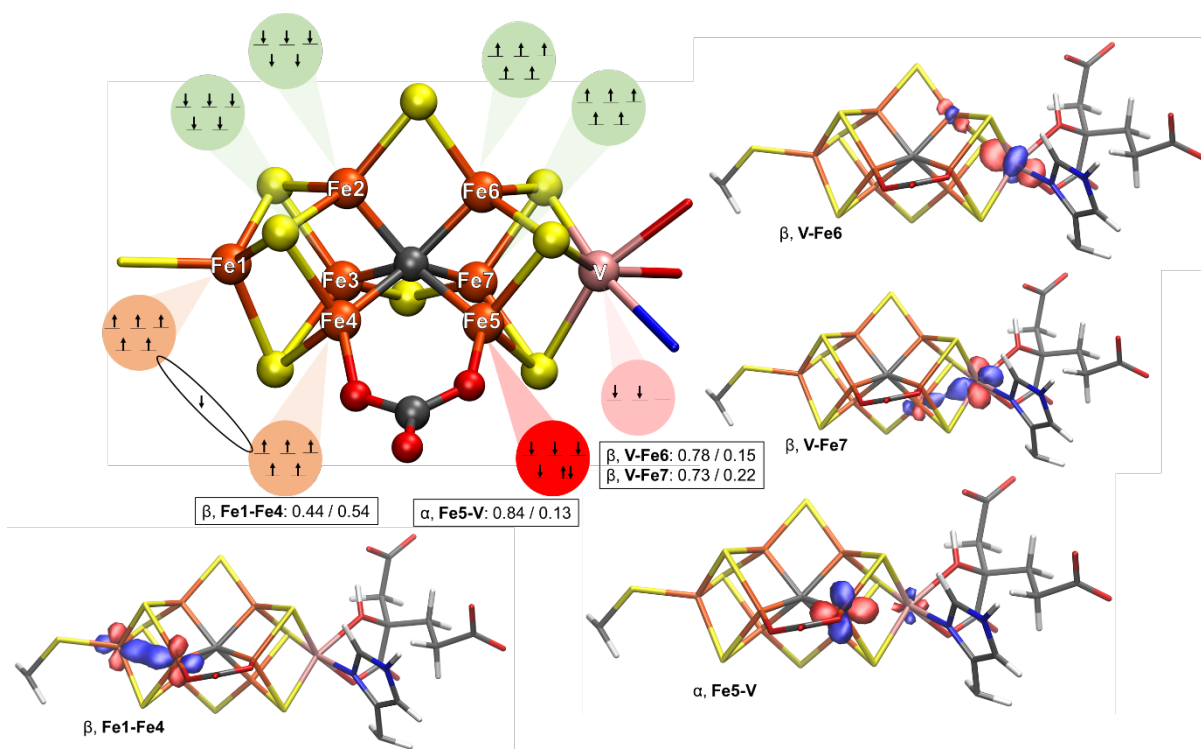


Figure S 23: The electronic structure of  $[V-CO_3]^0 M_S = 3/2$  BS7-235 model as interpreted by IAOIBOs. Shown are localized orbitals for the minority-spin electrons and the vanadium electrons and the atomic populations. Using 181 QM atom QM/MM model. Iso value of 0.1 was used to generate the figures of the orbitals.

The BS7 solutions: FeMoco vs. FeVco

As discussed in the manuscript, for FeVco the BS7-235 solution is considerably lower in energy (by 6 kcal/mol) than the analogous BS7-247 and BS7-346 solutions. For FeMoco the 3 BS7 solutions are all within 1 kcal/mol for FeMoco (Benediktsson, B.; Bjornsson, R. QM/MM Study of the Nitrogenase MoFe Protein Resting State: Broken-Symmetry States, Protonation States, and QM Region Convergence in the FeMoco Active Site. *Inorg. Chem.* **2017**, *56* (21), 13417–13429)

To separate out the effects of carbonate vs. sulfide, V vs. Mo and the different Fe redox state, we carried out calculations where the carbonate of FeVco was substituted by a sulfide, V was substituted by Mo or with both substitutions. When the carbonate ligand in FeVco is exchanged for a sulfide, the difference between the BS7-235 and the other BS7 solutions drops by  $\sim 4$  kcal/mol (Table S22) and the three BS7 solutions are much more similar in energy. A similar change in energy difference is, however, observed when the vanadium is substituted for molybdenum (and the negative charge is reduced by 1). Simultaneously substituting the vanadium for molybdenum and carbonate for sulfide in FeVco within the VFe protein matrix (essentially substituting FeVco for FeMoco), we see a further drop in the energy difference between the three BS7 solutions which is now less than 1 kcal/mol. Overall this suggests that the preference for BS7-235 in FeVco arises from both the carbonate ligand as well as the presence of V instead of Mo (and the reduced Fe environment).

Table S 21 The electronic energy of the three BS7 spin isomers of FeVco, FeVco-triS<sup>a</sup>, FeVco-Mo<sup>b</sup>, FeVco-triS-Mo<sup>c</sup> and FeMoco<sup>d</sup>, using a 57 QM atom QM/MM model for FeVco and 54 QM atom QM/MM model for FeMoco.

	FeVco	FeVco-triS <sup>a</sup>	FeVco-Mo <sup>b</sup>	FeVco-triS-Mo <sup>c</sup>	FeMoco <sup>d</sup>
BS7-235	0.0	0.0	0.0	0.0	0.7
BS7-247	6.0	2.0	2.3	0.3	1.1
BS7-346	6.5	1.6	1.4	0.6	0.0

<sup>a</sup>FeVco-triS: A 54 QM atom QM/MM optimized model (of the VFe protein) where carbonate has been substituted for a sulfide. [VFe<sub>7</sub>S<sub>9</sub>C]<sup>2-</sup> and M<sub>S</sub> = <sup>3</sup>/<sub>2</sub>

<sup>b</sup>FeVco-Mo: A 57 QM atom QM/MM optimized model (of the VFe protein) where vanadium has been substituted for a molybdenum. [MoFe<sub>7</sub>S<sub>8</sub>C(CO<sub>3</sub>)] and M<sub>S</sub> = <sup>3</sup>/<sub>2</sub>

<sup>c</sup>FeVco-triS-Mo: A 54 QM atom QM/MM optimized model (of the VFe protein) where carbonate has been substituted for sulfide and vanadium has been substituted for molybdenum (essentially FeMoco within the VFe protein matrix). [MoFe<sub>7</sub>S<sub>9</sub>C] and M<sub>S</sub> = <sup>3</sup>/<sub>2</sub>

<sup>d</sup>FeMoco: A 54 QM atom QM/MM optimized model (of the MoFe protein) as previously described. [MoFe<sub>7</sub>S<sub>9</sub>C] and M<sub>S</sub> = <sup>3</sup>/<sub>2</sub>.

The energy difference between the BS7 solutions of FeVco is not very sensitive to the QM region size, however, the geometries of all BS7 solutions when optimized are systematically improved with respect to the 5NY6 X-ray structure (Table S20) as the QM region increases. The BS7-235 structure is still in best agreement with the 5N6Y X-ray structure.

Table S 22: Root-Mean-Square Deviations (in Å) of different QM/MM Optimized Geometries with the Possible FeVco structure compared to the Experimentally Determined Crystal Structure). The RMSD is defined as the deviation of the [VFe<sub>7</sub>S<sub>8</sub>C(XO<sub>3</sub>)] part with respect to both cofactors in the crystal structure.

Model	RMSD [Å]	Relative energy difference [kcal/mol]	V-Fe1 distance [Å] (crystal 7.11 Å)
BS7-235-57QM	0.080	0	7.11
BS7-247-57QM	0.101	6.00	7.15
BS7-346-57QM	0.096	6.53	7.10
BS235-83QM	0.083	0	7.09
BS7-247-83QM	0.098	5.58	7.10
BS7-346-83QM	0.091	5.52	7.12
BS7-235-181QM	0.076	0	7.05
BS7-247-181QM	0.088	5.27	7.11
BS7-346-181QM	0.089	6.13	7.09

Table S 23: The effect of geometry optimization on the relative energy difference of BS7 class of broken symmetry solutions.

BS	Geometry type	QM region	Relative energy difference [kcal/mol]
BS7-235	X-ray	57	0
BS7-247	X-ray	57	7.83
BS7-346	X-ray	57	8.18
BS7-235	QM/MM opt	57	0
BS7-247	QM/MM opt	57	6.00
BS7-346	QM/MM opt	57	6.53
BS7-235	QM/MM opt	83	0
BS7-247	QM/MM opt	83	5.58
BS7-346	QM/MM opt	83	5.52
BS7-235	QM/MM opt	181	0
BS7-247	QM/MM opt	181	5.27
BS7-346	QM/MM opt	181	6.13

## Protonation state of homocitrate

QM/MM calculations of FeVco ( $[\text{V-CO}_3]^{2-}$  model) with and without the alcohol group of homocitrate protonated were carried out. A comparison of the computed structures with the X-ray crystal structure (PDB ID: 5N6Y) reveal that the alcohol group is most likely protonated. This is consistent with our previous finding for FeMoco in MoFe protein Benediktsson, B.; Bjornsson, R. QM/MM Study of the Nitrogenase MoFe Protein Resting State: Broken-Symmetry States, Protonation States, and QM Region Convergence in the FeMoco Active Site. *Inorg. Chem.* **2017**, *56* (21), 13417–13429). and another study (Cao, L.; Caldararu, O.; Ryde, U. Protonation States of Homocitrate and Nearby Residues in Nitrogenase Studied by Computational Methods and Quantum Refinement. *J. Phys. Chem. B* **2017**, *121* (35), 8242–8262.)

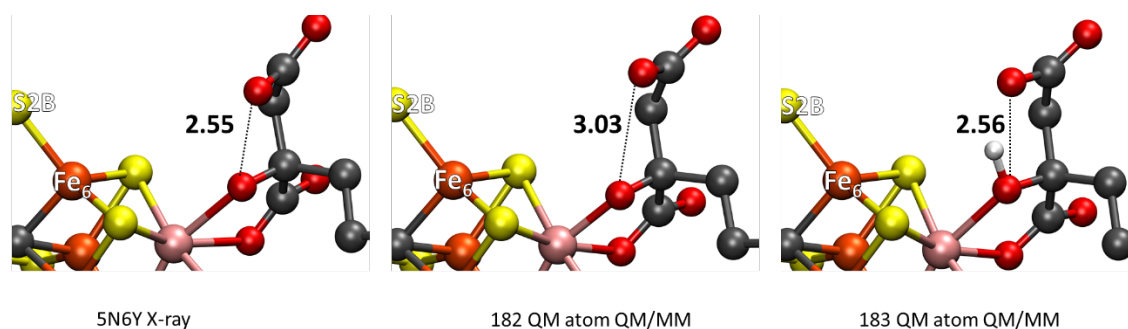


Figure S 24: Protonation state of the alcohol group of homocitrate of FeVco. Left: Close-up of the alcohol group of homocitrate of FeVco in the 5N6Y X-ray structure with the O-O distance between the alcohol group and the shorter carboxylate arm indicated. Middle: Computed structure with no proton present. Right: Computed structure with alcohol proton present.

## Protonated FeVco

Table S 24: Structural parameters comparing the average of the two FeVco cofactors of the X-ray structure to QM/MM calculated structures of protonated forms of the cofactors. HS2B: Sulfide S2B protonated, HS5A: Sulfide S5A protonated, 2XHCA: longer carboxylate arm of FeVco protonated. 58 QM atom QM/MM calculations.

	Crystal	HS2B	HS5A	2XHCA
Fe1-Fe2	2.71	2.69	2.69	2.72
Fe1-Fe3	2.66	2.64	2.61	2.65
Fe1-Fe4	2.58	2.66	2.66	2.63
V-Fe5	2.70	2.71	2.69	2.70
V-Fe6	2.77	2.74	2.82	2.90
V-Fe7	2.73	2.72	2.66	2.73
Fe2-Fe3	2.63	2.56	2.59	2.60
Fe2-Fe4	2.62	2.62	2.63	2.63
Fe3-Fe4	2.63	2.67	2.64	2.67
Fe5-Fe6	2.60	2.62	2.66	2.67
Fe5-Fe7	2.63	2.65	2.63	2.66
Fe6-Fe7	2.60	2.53	2.51	2.57
V-Fe1	7.11	7.12	7.10	7.15
C-Fe1	3.48	3.51	3.50	3.53
C-V	3.63	3.61	3.61	3.63
Fe2-Fe6	2.61	2.67	2.61	2.62
Fe3-Fe7	2.60	2.59	2.64	2.60
Fe4-Fe5	2.76	2.72	2.72	2.72
C-Fe2	1.95	2.01	2.01	2.03
C-Fe3	2.04	2.02	2.01	2.04
C-Fe4	2.02	2.00	1.99	2.00
C-Fe5	2.05	2.01	2.00	1.99
C-Fe6	1.98	2.02	2.02	2.02
C-Fe7	2.01	2.01	2.02	2.02
Fe4-OX	1.97	1.91	1.91	1.93
Fe5-Ocarb	1.93	1.91	1.91	1.92
Fe4-O-O-Fe5	-11.30	-2.57	-2.89	-5.06

V-Oalk	2.20	2.12	2.11	2.16
V-Ocarb	2.35	2.05	2.06	2.08
V-His	2.35	2.20	2.21	2.22
Fe1-Scys	2.16	2.26	2.26	2.29
Fe2-S2B	2.21	2.35	2.19	2.21
Fe6-S2B	2.17	2.34	2.19	2.19
Fe3-S5A	2.23	2.20	2.34	2.22
Fe7-S5A	2.27	2.20	2.34	2.20

### Unbound electrons

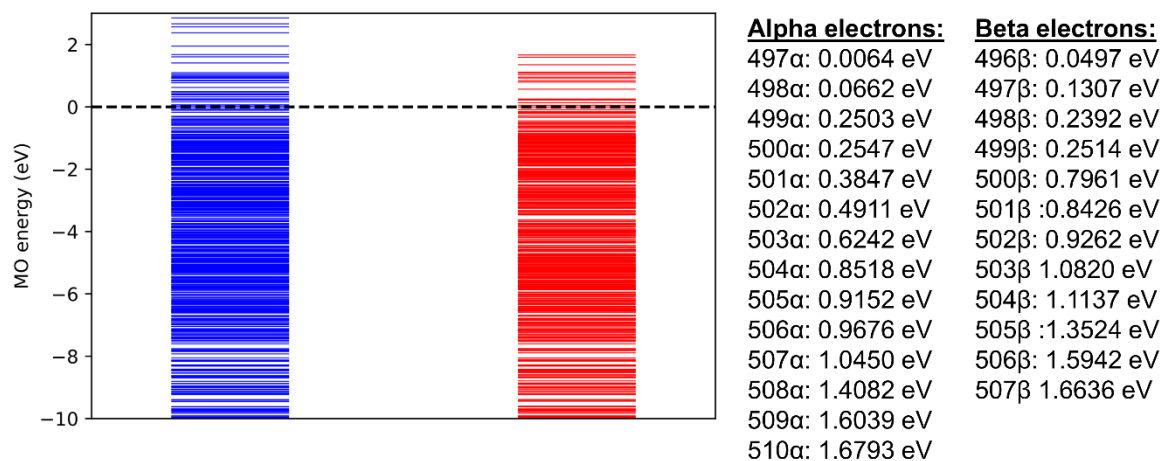


Figure S 25: MO diagram showing the occupied valence orbitals in the 181 QM atom QM/MM model of  $[\text{V-CO}_3]^{2-}$ . Orbitals with positive energies correspond to unbound electrons and are listed to the right.

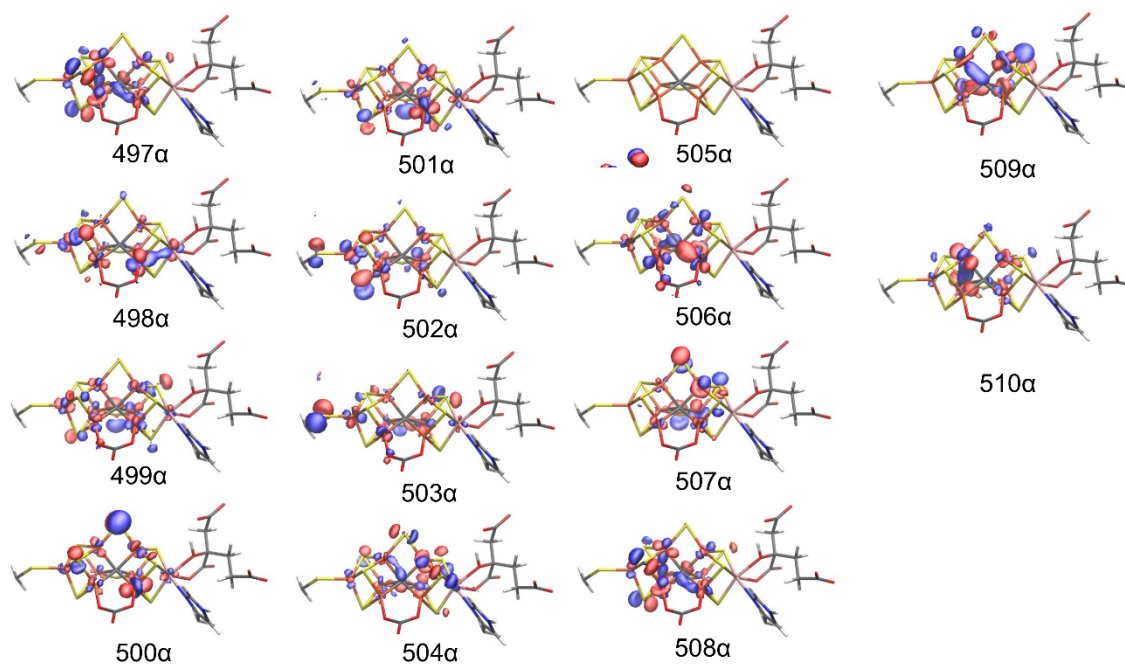


Figure S 26: Molecular orbitals of  $\alpha$  electrons that have positive orbital energies in a 181 QM atom QM/MM model of the  $[\text{V-CO}_3]^{2-}$  model. These high energy orbitals show mainly, but not only, sulfide and iron character

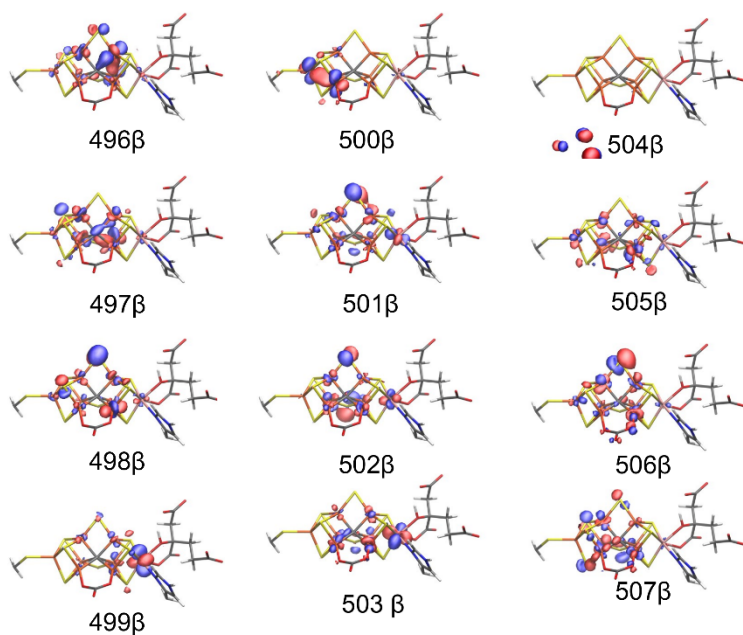


Figure S 27: Molecular orbitals of  $\beta$  electrons that have positive orbital energies in a 181 QM atom QM/MM model of the  $[\text{V-CO}_3]^{2-}$  model. These high energy orbitals show mainly, but not only, sulfide and iron character

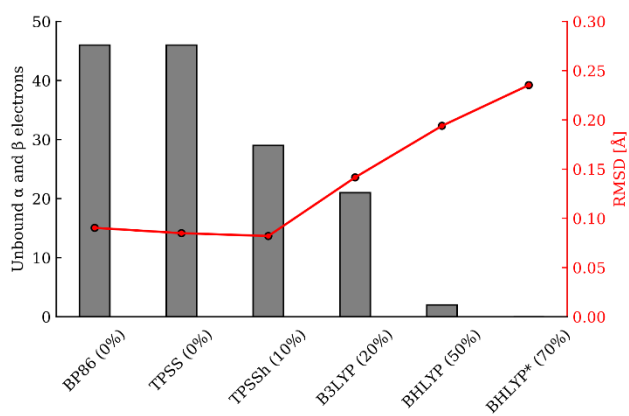
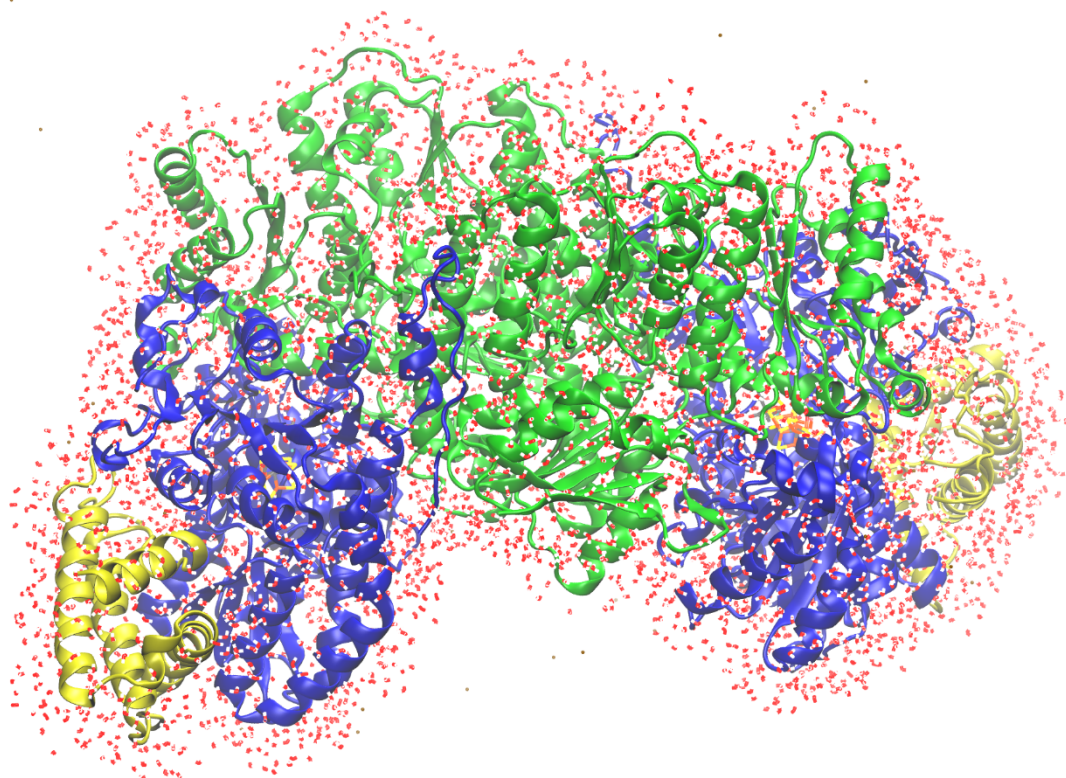


Figure S 28: The dependence of unbound electrons in the  $[\text{V-CO}_3]^{2-}$  resting state model on density functionals with different amount of HF exchange. Also shown (right y-axis) is the RMSD of the optimized cofactor with the respective functional. QM/MM model with a QM region size of 57 atoms. The RMSD is defined as the deviation of the  $[\text{VFe}_7\text{S}_8\text{C}(\text{XO}_3)]$  part with respect to both cofactors in the crystal structure.



Alternative QM/MM model of whole protein

The model is prepared similarly as the spherical QM/MM model. The difference between the two models is that instead of a spherical cut from the MD step, the whole protein is included as well as all water molecules within 3 Å of the protein matrix. This new QM/MM model 47 516 atoms in size.



*Figure S 29: The new QM/MM model (47 516 atoms) includes the whole VFe protein as well as sodium ion counterions and 3 Å thick water layer at the edge of the VFe protein.*

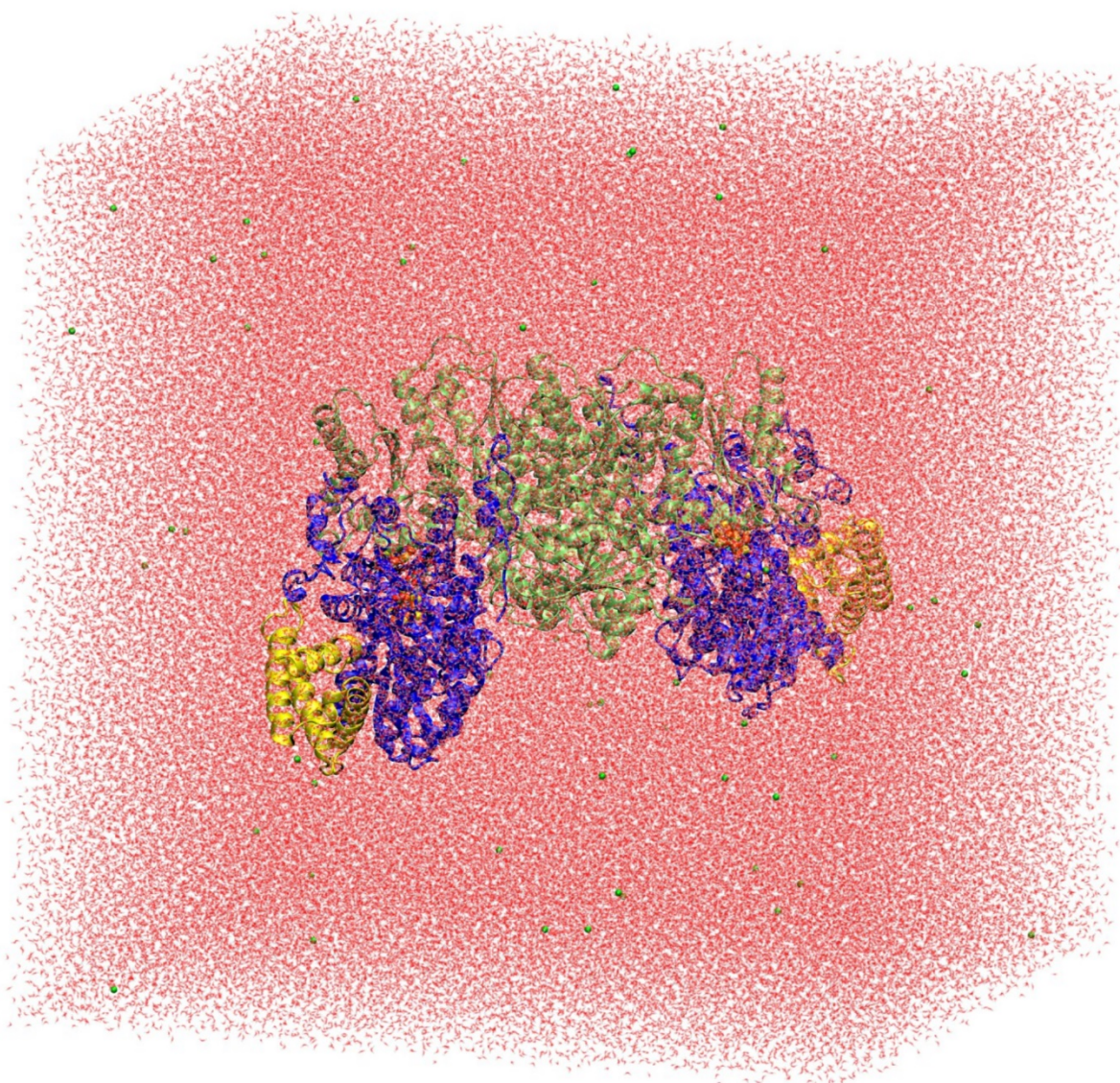


Figure S 30: *The 531 080 atom QM/MM model (full box from the MM setup).*



Table S 25: Mulliken spin populations of the FeVco  $[VFe_7S_8C(CO_3)]^{2-}$  model using 47 516 atom and 531 080 atom QM/MM model setups.

QM atoms	57		181	
	47 516	531 080	47 516	531 080
V	-1.650	-1.649	-1.634	-1.630
Fe1	3.477	3.479	3.459	3.462
Fe2	-3.292	-3.292	-3.286	-3.288
Fe3	-3.290	-3.293	-3.274	-3.277
Fe4	3.428	3.427	3.387	3.388
Fe5	-3.218	-3.218	-3.187	-3.186
Fe6	3.289	3.288	3.291	3.289
Fe7	3.221	3.222	3.210	3.208
S1A	0.183	0.182	0.200	0.199
S2A	-0.014	-0.019	-0.013	-0.018
S4A	0.164	0.161	0.169	0.167
S1B	0.084	0.084	0.079	0.079
S3B	0.273	0.270	0.279	0.275
S4B	0.106	0.105	0.099	0.098
S2B	0.012	0.015	0.009	0.013
S5A	0.014	0.019	-0.008	-0.004
C*	0.059	0.061	0.055	0.057
C	-0.001	0.000	-0.005	-0.005
O3	0.041	0.043	0.026	0.027
O1	-0.020	-0.022	-0.008	-0.009
O2	-0.001	-0.001	0.000	0.000

Table S 26: Comparison of metal-metal distances in different X-ray structures of MoFe: the deviation of metal-metal distances of each FeMoco unit in various X-ray structures to one FeMoco unit in the 1.0 Å resolution crystal structure (PDB ID: 3U7Q).

Resolution [Å]	1.00	1.16	1.16	1.16	1.16	1.43	1.43	QM/MM 367 QM atoms <sup>d</sup>
PDB ID	3U7Q	1M1N <sup>b</sup>	1M1N <sup>b</sup>	1M1N <sup>b</sup>	1M1N <sup>b</sup>	4TKU <sup>c</sup>	4TKU <sup>c</sup>	
FeMoco unit number <sup>a</sup>	2	1	2	3	4	1	2	
Fe1-Fe2	-0.012	-0.004	0.008	-0.012	-0.001	-0.006	0.001	0.021
Fe1-Fe3	0.005	-0.004	0.010	-0.001	-0.002	-0.003	-0.001	0.034
Fe1-Fe4	-0.007	0.004	0.002	-0.006	-0.005	0.004	0.007	0.013
Mo-Fe6	0.007	0.002	0.004	0.011	-0.001	0.017	0.015	0.025
Mo-Fe7	0.005	-0.005	-0.002	-0.007	-0.006	0.014	0.005	0.055
Mo-Fe5	0.003	-0.003	0.001	0.014	0.001	0.010	0.004	0.022
Fe2-Fe3	0.002	-0.001	0.013	-0.002	0.009	0.008	0.005	0.019
Fe3-Fe4	-0.002	-0.003	-0.002	0.000	-0.009	0.005	-0.002	0.028
Fe2-Fe4	0.000	0.001	0.013	-0.003	0.003	0.017	0.015	0.026
Fe6-Fe7	0.003	-0.004	0.015	0.017	0.007	0.013	0.001	0.040
Fe5-Fe6	0.001	-0.006	0.002	0.018	0.000	0.001	-0.007	-0.002
Fe5-Fe7	-0.002	0.004	0.006	0.011	0.008	0.004	-0.008	0.010
Fe2-Fe6	-0.003	-0.004	-0.001	0.003	0.003	-0.004	-0.007	-0.010
Fe3-Fe7	-0.001	0.026	0.028	0.031	0.032	0.035	0.032	0.003
Fe4-Fe5	-0.006	-0.032	-0.041	-0.041	-0.035	-0.030	-0.034	-0.011
Absolute average deviation	0.004	0.007	0.010	0.012	0.008	0.011	0.010	0.021

<sup>a</sup> As the MoFe protein is a dimer, there are two units of FeMoco per protein.

<sup>b</sup> In the case of 1M1N, there are two units of the MoFe protein in the X-ray structure and therefore 4 units of FeMoco (Reference: Einsle, O. Nitrogenase MoFe-Protein at 1.16 Å Resolution: A Central Ligand in the FeMo-Cofactor. *Science*. **2002**, 297 (5587), 1696–1700. <https://doi.org/10.1126/science.1073877>.)

<sup>c</sup> As the MoFe protein is a dimer, there are two units of FeMoco per protein (Reference: Spatzal, T.; Perez, K. A.; Einsle, O.; Howard, J. B.; Rees, D. C. Ligand Binding to the FeMo-Cofactor: Structures of Co-Bound and Reactivated Nitrogenase. *Science*. **2014**, 345 (6204), 1620–1623.)

<sup>d</sup> From a previous study by us (Reference: Benediktsson, B.; Bjornsson, R. QM/MM Study of the Nitrogenase MoFe Protein Resting State: Broken-Symmetry States, Protonation States, and QM Region Convergence in the FeMoco Active Site. *Inorg. Chem.* **2017**, 56 (21), 13417–13429)